

A microfluidic device based on droplet storage for screening solubility diagrams

Philippe Laval,* Nicolas Lisai, Jean-Baptiste Salmon and Mathieu Joanicot

Received 18th January 2007, Accepted 2nd April 2007

First published as an Advance Article on the web 20th April 2007

DOI: 10.1039/b700799j

This work describes a new microfluidic device developed for the rapid screening of solubility diagrams. In several parallel channels, hundreds of nanolitre volume droplets of a given solution are first stored with a gradual variation in the solute concentration. Then, the application of a temperature gradient along these channels enables us to read directly and quantitatively phase diagrams, concentration *vs.* temperature. We show, using a solution of adipic acid, that we can measure ten points of the solubility curve in less than 1 hr and with only 250 μL of solution.

1. Introduction

Chemistry, biology, and pharmacology are always facing more complex systems depending on multiple parameters. Therefore their complete investigations take time and require significant amounts of products. In this context, robotic fluidic workstations have already met with great success and proved their efficiency, for instance in genome sequencing and analysis.¹ However, these instruments remain very expensive, need costly labour, and the volumes involved ($\leq\text{mL}$) are still too large for some specific applications (*e.g.* proteomics).^{2,3}

Nowadays, other high throughput techniques based on microfluidics^{4,5} can offer suitable alternative solutions for the development of rapid screening tools. Microfluidic devices are now largely used in biological and chemical fields for multiple applications⁶ like molecular separations and cell sorting,⁷ polymerase chain reaction,^{8,9} rapid micromixing and analysis of chemical reactions...^{10–13} Moreover, the development of microvalves and micromixers has made possible the production of highly integrated systems which can be used to address individually hundreds of reaction chambers.¹⁴ These devices are well adapted to carry out high throughput screening of phase diagrams, particularly in the case of protein crystallization investigation. However, their fabrication and multiplexing are still complicated. Another possible strategy is the use of droplets playing the role of nanolitre sized reaction compartments. These droplets can be produced in specific microfluidic geometries,¹⁵ and their volume and chemical composition can be fixed in a controlled way. In addition, they also allow a rapid mixing of the different compounds, help prevent hydrodynamic dispersion and cross contamination, and can be stored in microchannels (see ref. 16 and references cited therein). Such a strategy has already proved to be useful for crystallization studies, *e.g.*, screening of protein crystallization conditions,^{17,18} or crystal nucleation kinetic measurements.¹⁹

Fig. 1 summarizes the main insights of our work. We have engineered a new microfluidic chip that allows the direct and

quantitative reading of two-dimensional diagrams. Hundreds of nanolitre sized droplets of different chemical compositions can be stored in parallel microchannels, and a temperature gradient applied along these channels enables us to obtain a two-dimensional array of droplets of different concentrations and temperatures. For solubility diagram screening, droplets containing a given solute are first stored with a gradual variation of concentration. Then, crystallization in the droplets is induced by cooling, and finally, the application of an adequate temperature gradient dissolves crystals in droplets whose temperature is higher than their solubility temperature. As a result, we directly read the limit between droplets with and without crystals, as shown in Fig. 1(c), which gives the solubility temperatures of the solution at the different concentrations.

In the materials and methods section, we describe the microfluidic device, the method used to store the droplets in the channels, and the temperature control setup. We also characterize the concentration and temperature gradients. In the last section, we present an experimental protocol to measure quantitatively solubility diagrams using this device. We demonstrate its efficiency by measuring, with only 250 μL of solution, the solubility curve of an organic compound.

2. Materials and methods

2.1. Microfabrication

The microfluidic device is fabricated in poly(dimethylsiloxane) (PDMS) by using soft-lithographic techniques.²⁰ PDMS (Silicone Elastomer Base, Sylgard 184; Dow Corning) is moulded on master fabricated on a silicon wafer (3-Inch-Si-Wafer; Siegert Consulting *e.k.*) using a negative photoresist (SU-8 2100; MicroChem). To make moulds of 500 μm height, we spin successively two 250 μm thick SU-8 layers on the wafer. After each spin coating process, the wafer is soft-baked (10 min/65 $^{\circ}\text{C}$ and 60 min/95 $^{\circ}\text{C}$). Photolithography is used to define negative images of the microchannels. Eventually, the wafer is hard-baked (25 min/95 $^{\circ}\text{C}$) and developed (SU-8 Developer; MicroChem). A mixture 10 : 1 of PDMS is moulded on the SU-8 master described above (65 $^{\circ}\text{C}$ /60 min). The cross-linked PDMS layer is then peeled off the mould and

LOF, unité mixte Rhodia–CNRS–Bordeaux 1, 178 avenue du Docteur Schweitzer, F-33608, Pessac cedex, France.
E-mail: philippe.laval-exterieur@eu.rhodia.com

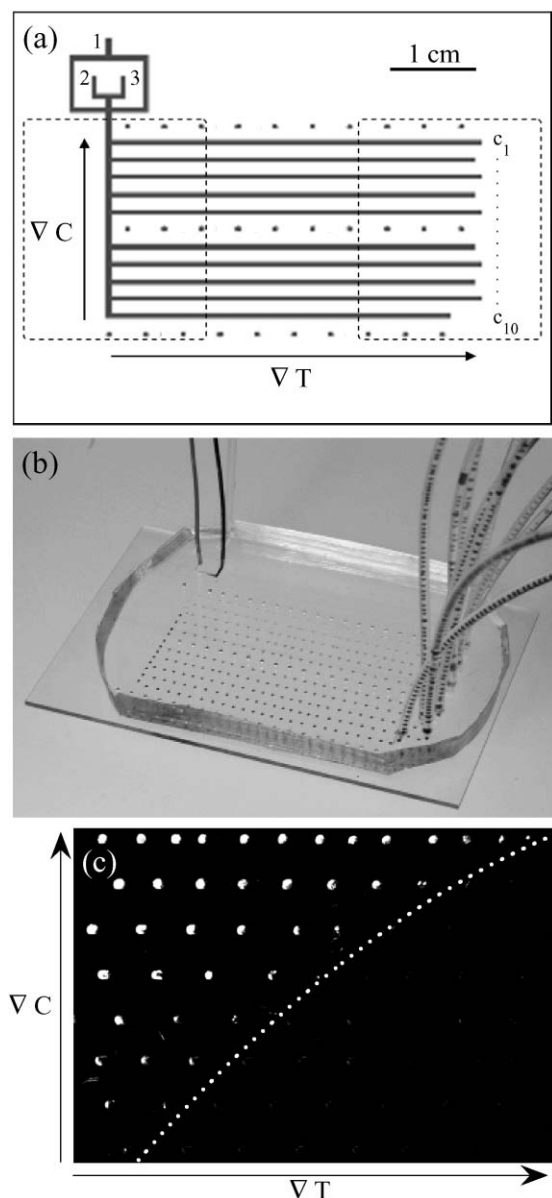


Fig. 1 (a) Design of the microfluidic device (channels width $500\ \mu\text{m}$). Silicone oil is injected in inlet 1 and aqueous solutions in inlets 2 and 3. The two dotted areas indicate the positions of the two Peltier modules used to apply temperature gradients ∇T . The three lines of dots mark the positions of temperature measurements. (b) Picture of the microfluidic chip made of PDMS sealed with a glass slide ($76 \times 52\ \text{mm}^2$) to improve clarity. Droplets containing a coloured dye at different concentrations are stored in the ten parallel channels. (c) Example of direct reading of a solubility diagram. The droplets contain an organic solute. The dotted line bounding droplets containing crystals gives an estimation of the solubility limit (see Results section for details).

holes for the inlets and outlets (1/32 and 1/16 in od) are punched into the material. Then, the PDMS surface and a clean silicon wafer surface (3-Inch-Si-Wafer; $500\ \mu\text{m}$; Siegart Consulting e.k.) are activated for 2 min in a UV ozone apparatus (UVO Cleaner, Model 144AX; Jelight) and brought together. Finally, the device is placed at $65\ ^\circ\text{C}$ for 2 hr to improve the sealing.

2.2. Droplet storage protocol

The device, presented in Fig. 1(a), is composed of three inlets and ten outlets located at the extremities of channels c_1 to c_{10} . As shown in Fig. 1(b), each outlet is connected to a $\approx 20\ \text{cm}$ long rigid tubing (FEP 1/16 in) ending with a piece of soft PVC tubing (Nalgene, $\approx 5\ \text{cm}$ long) inserted into an automated pinch electrovalve (105S-01059P; Asco Joucomatic). Thanks to this system, each outlet can be independently closed or opened by pinching or not pinching the corresponding PVC tubing. However, the pinching out of a tube leads to a liquid displacement. To minimize the subsequent liquid disturbance in the microchannels, the electrovalves are placed close to the rigid ones, and the hydrodynamic resistance after the electrovalves is kept as weak as possible using large tubing.

Silicone oil (500 cSt; Rhodorsil) is injected into inlet 1 at constant flow rate $Q_1 \approx 3\ \text{mL hr}^{-1}$, and aqueous phases are injected at flow rates Q_2 and Q_3 ranging from 0 to about $1\ \text{mL hr}^{-1}$, into inlets 2 and 3, respectively. All liquids are injected with syringe pumps (PHD 2000 infusion; Harvard Apparatus). At the intersection between the oil and the aqueous streams, monodisperse droplets of the aqueous phase in oil are continuously produced.²¹ Both the droplet volume (about 100–300 nL) and their production frequency (typically between one and ten droplets per second) can be tuned by the ratio of oil to aqueous phase flow rates. The droplet composition is monitored by the ratio Q_2/Q_3 .

Thanks to the possible opening and closing of each outlet, we can store droplets of given aqueous compositions in the different storage channels c_i . Several steps are necessary to perform such a filling. First, all the channels are initially filled with silicone oil. Secondly, the outlet of channel c_1 is opened and all the others are closed. In this configuration, all the droplets of a given composition flow through c_1 . Finally, once the flow is stable, the outlet of c_1 is suddenly closed and simultaneously, the outlet of channel c_2 is opened. All the droplets previously present in c_1 stay immobilized whereas the other droplets, whose composition can be changed, flow through c_2 . Successively, in the same way, we can store droplets of various compositions in all channels c_i .

2.3. Chemical composition control

For solubility investigations, the control of the concentrations in the droplets is crucial. However, because of PDMS elasticity and syringe pump precision, an inaccuracy in droplet concentration remains. To estimate this error, we have performed investigations with a confocal Raman microscope (HR800 Horiba; Jobin-Yvon). A $50\times$ microscope objective was used for focusing a 532 nm wavelength laser beam in the droplets, and for collecting Raman scattered light, subsequently dispersed with a grating of 600 lines per millimetre. To minimize the out-of-focus background signals, we fixed the confocal pinhole at $500\ \mu\text{m}$. Experiments were performed on droplets made of two initial aqueous solutions of $\text{K}_4\text{Fe}(\text{CN})_6$ (0.5 M) and $\text{K}_3\text{Fe}(\text{CN})_6$ (0.5 M) injected in inlets 2 and 3, respectively. These two compounds display strong and distinct Raman signals.²²

Fig. 2 shows three Raman spectra measured in droplets containing different concentration ratios $R_C = [\text{K}_4\text{Fe}(\text{CN})_6]/[\text{K}_3\text{Fe}(\text{CN})_6]$. The two bands centred at 2060 and $2095\ \text{cm}^{-1}$

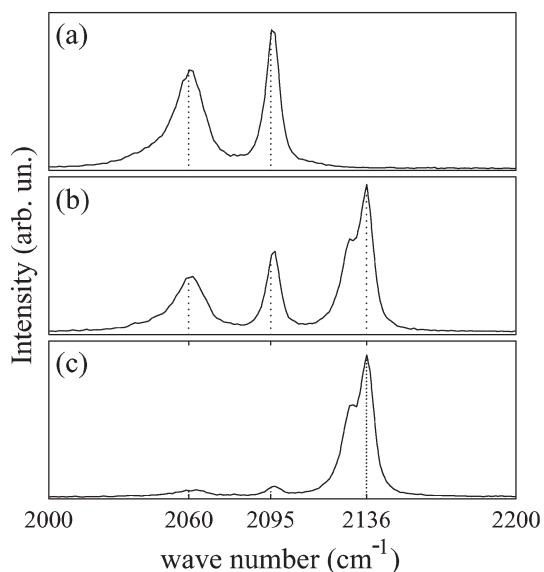


Fig. 2 Raman spectra of droplets containing different concentration ratios R_C of potassium ferrocyanide $K_4Fe(CN)_6$ and potassium ferricyanide $K_3Fe(CN)_6$. (a) $R_C = 0$ (b) $R_C = 1$ (c) $R_C = 9$.

correspond to $K_3Fe(CN)_6$ and the one at 2136 cm^{-1} corresponds to $K_4Fe(CN)_6$. The concentration of each compound can be probed from the area under their specific Raman bands by:

$$A_i = K_i C_i t V, \quad (1)$$

where A_i is the area under the Raman band of the compound i , C_i its concentration, K_i a specific constant, t the acquisition time, and V the analysis volume. As a consequence, the ratio R_A of the Raman bands areas of $K_4Fe(CN)_6$ and $K_3Fe(CN)_6$ is proportional to the concentration ratio R_C , and does not depend on the acquisition parameters.

In order to optimize the filling protocol, we use first Raman microscopy to follow the kinetics of the concentration stabilization in the droplets after a sudden change in the aqueous phase flow rates. Indeed, due to the PDMS elasticity and the injection system (syringe pumps), the finite response time of the device does not allow instantaneous change of the concentrations. To estimate this response time, we have performed the following experiment: for $t < 0\text{ s}$, $Q_2 = 0$ and $Q_3 = 500\text{ }\mu\text{L hr}^{-1}$, and for $t > 0\text{ s}$, $Q_2 = Q_3 = 250\text{ }\mu\text{L hr}^{-1}$. Droplets flow first through channel c_1 which is closed after 30 s. Then, droplets are stored in five other channels after 1, 2, 4, 6, and 10 min. Thus, Raman spectra obtained from the droplets in the different channels enable us to follow the evolution of R_A as a function of time after the flow rates change. Fig. 3(a) shows it reaches almost a constant value after 60 s, meaning the concentrations become stable after this time. Such measurements illustrate that 20 min long protocols are efficient to store droplets of desired compositions in the ten channels ($\approx 2\text{ min}$ per channel).

A second series of experiments was performed to estimate and characterize the concentration gradient we can apply in the device. The storage channels are filled with droplets of different concentrations in $K_3Fe(CN)_6$ and $K_4Fe(CN)_6$ set

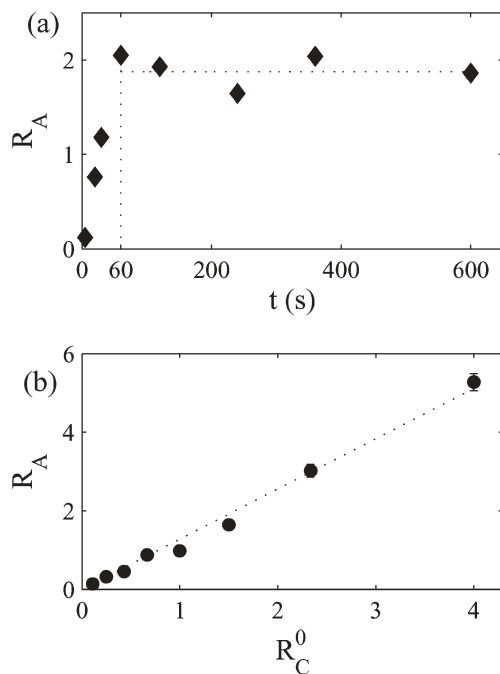


Fig. 3 (a) Evolution of the ratio R_A in the droplets after a sudden change of the aqueous solutions' flow rates Q_2 and Q_3 . Before $t = 0\text{ s}$, $Q_2 = 0$ and $Q_3 = 500\text{ }\mu\text{L hr}^{-1}$. For $t > 0\text{ s}$, $Q_2 = Q_3 = 250\text{ }\mu\text{L hr}^{-1}$. Between 5 and 30 s, R_A are obtained from three single droplets in channel c_1 . After $t = 60\text{ s}$, each point is a mean value calculated on several droplets in a given channel. (b) Concentration ratio R_A in droplets as a function of the concentration ratio R_C^0 determined from the aqueous solutions flow rates. The dotted line corresponds to the linear fit of the data.

from the flow rates. In each channel c_i , to reach a stable droplet composition, we maintain the flow for 90 s before closing the outlet to store them [see Fig. 3(a)]. By measuring the Raman spectra of the droplet composition in the different channels, we obtain the ratio R_A as a function of the theoretical ratio $R_C^0 = Q_2/Q_3$. The error bar corresponds to the standard deviation of the measurements performed on the droplets in a given channel. As can be seen in Fig. 3(b), a linear relationship between R_A and R_C^0 is observed as expected. Deviations of a few percents around the linear law are probably due to the Raman measurements uncertainties, to the accuracy of the injection system, and also to the PDMS elasticity.

These Raman measurements demonstrate that with the developed protocol, we are able to store hundreds of droplets in ten channels in about 20 min, while consuming less than a few hundreds of μL of solution. We believe that more rigid and smaller microdevices combined with an even more reactive injection system will decrease significantly the amount of liquids used when filling the channels. Other strategies involving, for instance, droplet generation thanks to integrated microvalves,²³ may also be proved useful in decreasing the required volumes of solution.

2.4. Temperature control

The temperature field of the chip is controlled with two Peltier modules ($30 \times 30 \times 3.3\text{ mm}^3$; CP1.4-71-06L; Melcor) placed

underneath the wafer at positions marked by the two dotted areas on Fig. 1(a). Since the two Peltier modules are independent, we can heat or cool the device, and also apply important temperature gradients. We use a silicon wafer as chip support to optimize thermal transfers and thus to create regular temperature gradients along the storage channels. Thin thermocouples (type K, 76 μm od, 5SRTC-TTKI-40-1M; Omega) measure the temperature of the device along three series of positions parallel to the storage channels. The first series is placed above c_1 , the second one between c_5 and c_6 , and the third one below c_{10} [see Fig. 1(a)]. To reach the maximal precision on liquid temperature measurements inside the channels, the thermocouples are inserted in holes previously punched through the PDMS layer and filled with silicone oil. Thermocouples signals are processed with a data acquisition instrument (USB-9161; National Instruments) and LabView software. Fig. 4(a) shows we are able to apply easily temperature gradients up to 45 $^\circ\text{C}$ on 5 cm. To estimate the temperature at any positions along the storage channels, we perform a longitudinal and transverse linear interpolation of the three series of measurements. The final profile obtained after such interpolation is depicted in Fig. 4(b). Note that the temperature is not perfectly homogeneous transversely to the storage channels. This is due to the size of the Peltier module as compared with the size of the droplet storage area: a

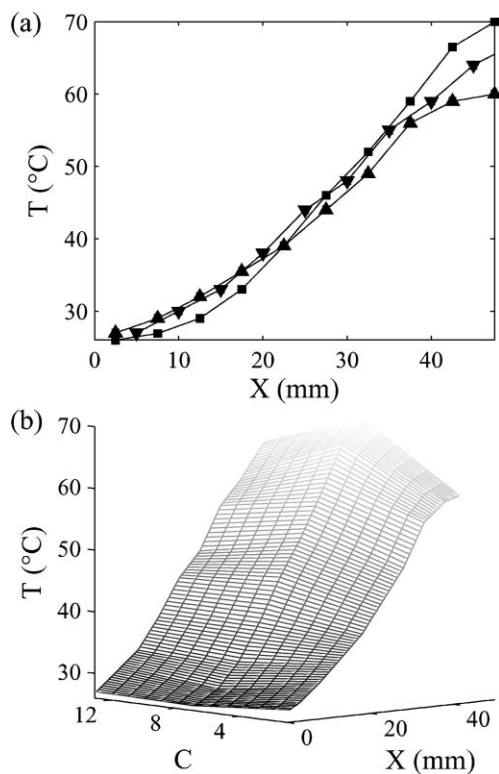


Fig. 4 Temperature profiles of the chip for a given temperature gradient. (a) Temperatures measured along the storage channels with thermocouples inserted through the PDMS layer at different positions shown on Fig. 1(a). (▲) Measurement series above channel c_1 ; (■) series between c_5 and c_6 ; (▼) series below c_{10} . (b) Interpolated temperature profile of the chip.

smaller storage area, or larger Peltier modules, would give homogeneous temperature profiles along the transverse direction of the channels.

3. Results

In the previous section we have shown that our microdevice allows us to build a two-dimensional array of droplets with both concentration and temperature gradients. We now present an application of this chip by measuring the solubility curve of an organic solute.

Such measurements are carried out with an adipic acid solution previously prepared in a beaker. It is made of 10.14 g of adipic acid (99%; Aldrich) in 50.66 g of de-ionized water. The solubility temperature of the solution is 63 $^\circ\text{C}$. To avoid any crystallization before the droplets formation, the syringe containing the solution and the corresponding tubing are heated at about 65 $^\circ\text{C}$ with two flexible heaters (Minco) controlled with temperature controllers (Minco). A stereo microscope (SZX12; Olympus) with an objective (DF PLFL 0.5 \times PF; Olympus) enables us to observe the device during the solubility study.

We inject the adipic acid solution in inlet 2 and de-ionized water in inlet 3. By changing the flow rate ratio we fill the storage channels with droplets whose concentration in adipic acid varies from 20 g per 100 g of water in channel c_1 down to 6 g per 100 g of water in c_{10} . The massic concentration C in the droplets is calculated according to:

$$C = \frac{C^0}{1 + (1 + C^0)Q_3/Q_2} \quad (2)$$

where C^0 is the massic concentration of the initial adipic acid solution and, Q_2 and Q_3 the respective flow rates of the solution and water (we checked that density variations induced by the presence of adipic acid are negligible). The microfluidic chip is kept at about 65 $^\circ\text{C}$ using the Peltier modules to avoid any crystallization during the droplet storage. Before stopping the droplets in a channel, we maintain it open for 90 s for flow stabilization. In these conditions, the total filling of the ten channels is reached in less than 20 min and only 250 μL of solution is spent.

After the droplet storage crystallization is induced by cooling. Note that the mean time of crystal nucleation is inversely proportional to the reactor volume. Indeed, the nucleation frequency is given by $1/JV$ where J is the nucleation rate which does not depend on the volume V of the reactor (see refs. 19,24–26 and references cited therein). Crystal nucleation in a droplet of 100 nL is thus 10^4 times longer than in a vial of 1 mL. To reduce such a long induction time we apply a strong cooling to increase the supersaturation significantly. In our case, down to ≈ -5 $^\circ\text{C}$, crystals appear in all the droplets after a few minutes.

To obtain the solubility curve directly on the chip, we then apply a temperature gradient between 32 and 65 $^\circ\text{C}$ after the crystallization step. Crystals dissolve in all the droplets whose temperature is higher than their solubility temperature. In the other droplets, crystals are partly solubilized but still exist (the equilibrium is reached in about 20 min). Typical images of the storage area are presented in Fig. 5. Since adipic acid

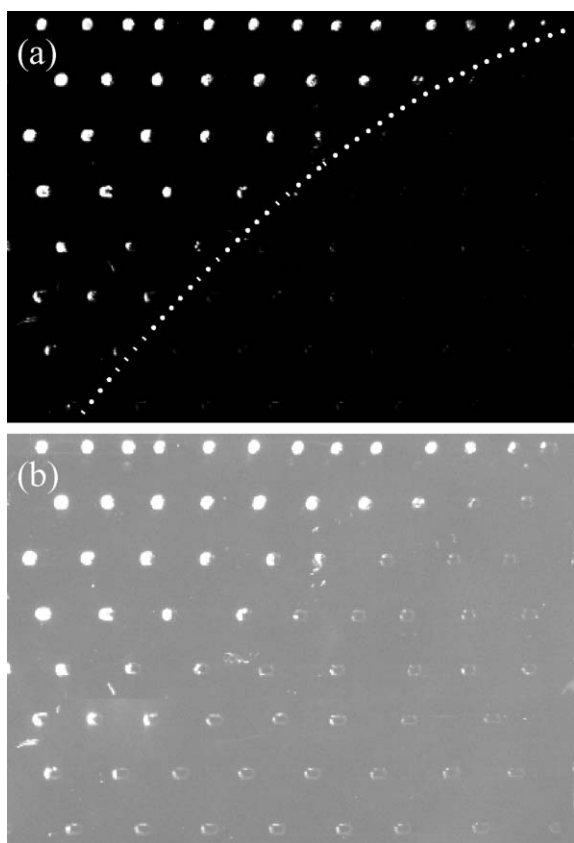


Fig. 5 Images of part of the storage area obtained under crossed polarizers. Droplets of adipic acid solution are stored in the channels. The concentration in adipic acid was gradually changed between the upper and the bottom channels. After crystallization of all the droplets, a temperature gradient is applied (low temperature on the left and high temperature on the right). (a) The dotted line separating droplets containing crystals from empty droplets gives an estimation of the solubility limit. (b) Same image but with a different contrast displaying the droplet positions.

crystals have birefringent properties, they are easily detected under crossed polarizers. The smallest detectable crystal size is about $50 \times 50 \mu\text{m}^2$ at the magnification used. Fig. 5(a) enables us to directly observe the limit of crystal presence. Using interpolated temperature profiles such as the one displayed in Fig. 4 allows us to estimate the solubility temperatures for all ten concentrations (we choose them in the middle of the two successive droplets with and without crystals). Fig. 6 presents such solubility temperatures measured with our microfluidic device. The error corresponds to the temperature difference between the two droplets enclosing the solubility limit positions. These results are in good agreement with data obtained from literature.²⁷

Naturally, the errors involved in such measurements depend on the distance between two successive droplets, and on the amplitude of the temperature gradient. In our case, a temperature gradient of $0.7 \text{ }^\circ\text{C mm}^{-1}$ and a typical distance of 3 mm between the two droplets gives an error of $\pm 1 \text{ }^\circ\text{C}$. The application of smaller temperature gradients and the reduction of the distance between two successive droplets would give better accuracy on the solubility limit.

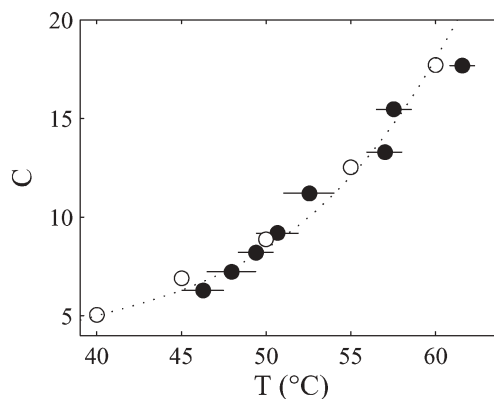


Fig. 6 (●) Solubility of adipic acid in water measured in the case of a temperature gradient of $0.7 \text{ }^\circ\text{C mm}^{-1}$. (○) Solubility data from literature: the dotted line is a guideline for the eyes.

For the moment, the maximum temperature which can be investigated is limited by the evaporation of water through the PDMS layer.²⁸ Simple measurements show that the volume of an aqueous droplet stored in our device at $60 \text{ }^\circ\text{C}$ decreases by $\approx 10\%$ in 4 hr. Such an effect is negligible for the experiments described above (droplet filling time 20 min at $65 \text{ }^\circ\text{C}$), but may explain the small discrepancy observed on Fig. 6 at high temperature. We believe that the use of non-permeable materials such as glass, instead of PDMS, could easily broaden the possibilities offered by our system.

4. Conclusion

In this work we have presented a new microfluidic tool to perform rapid screening of solubility diagrams. The device enables us to store hundreds of droplets ($\approx 100 \text{ nL}$) of various chemical compositions in parallel microchannels, and to apply large temperature gradients. We have demonstrated, using a model system (adipic acid in water), that we could easily and directly access ten simultaneous measurements of the solubility curve on a large temperature range in less than 1 hr, and with only $250 \mu\text{L}$ of solution. To conclude, we believe our device is a suitable tool for solubility diagram screening, more rapid, with a better temperature control, and cheaper than classical robotic workstations. Such a microfluidic tool may also be useful for many other applications, where two-dimensional screening, temperature vs. composition, is required.

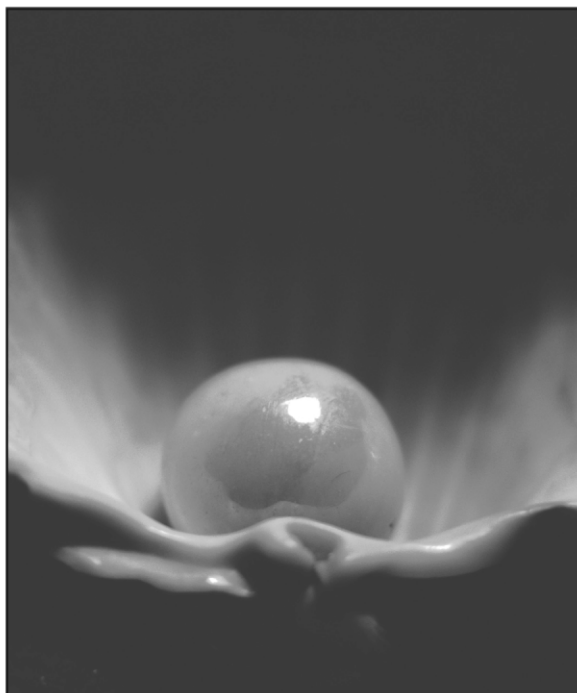
Acknowledgements

We gratefully thank G. Cristobal, J. Krishnamurti, J. Leng, and F. Sarrazin for fruitful discussions and critical reading of this manuscript. We also acknowledge *Région Aquitaine* for funding and support, and the *Atelier Mécanique* of the CRPP for their technical help.

References

- 1 G. H. W. Sanders and A. Manz, *Trends Anal. Chem.*, 2000, **19**, 364.
- 2 J. R. Luft, J. Wolfley, I. Jurisica, J. Glasgow, S. Fortier and G. T. DeTitta, *J. Cryst. Growth*, 2001, **232**, 591.
- 3 D. L. Chen and R. F. Ismagilov, *Curr. Opin. Chem. Biol.*, 2006, **10**, 226.

- 4 H. A. Stone, A. D. Stroock and A. Ajdari, *Annu. Rev. Fluid. Mech.*, 2004, **36**, 381.
- 5 T. M. Squires and S. R. Quake, *Rev. Mod. Phys.*, 2005, **77**, 977.
- 6 T. Vilckner, D. Janasek and A. Manz, *Anal. Chem.*, 2004, **76**, 3373.
- 7 N. Minc, C. Fütterer, K. D. Dorfman, A. Bancaud, C. Gosse, C. Goubault and J. L. Viovy, *Anal. Chem.*, 2004, **76**, 3770.
- 8 J. Khandurina and A. Guttman, *J. Chromatogr., A*, 2002, **943**, 159.
- 9 M. Chabert, K. D. Dorfman, P. de Cremoux, J. Roeraade and J.-L. Viovy, *Anal. Chem.*, 2006, **78**, 7722.
- 10 A. D. Stroock, S. K. Dertinger, A. Ajdari, I. Mezic, H. A. Stone and G. M. Whitesides, *Science*, 2002, **295**, 647.
- 11 E. M. Chan, A. P. Alivisatos and R. A. Mathies, *J. Am. Chem. Soc.*, 2005, **127**, 13854.
- 12 J.-B. Salmon, C. Dubrocq, P. Tabeling, S. Charier, D. Alcor, L. Jullien and F. Ferrage, *Anal. Chem.*, 2005, **77**, 3417.
- 13 S. A. Khan, A. Gunther, M. A. Schmidt and K. F. Jensen, *Langmuir*, 2004, **20**, 8604.
- 14 T. Thorsen, S. J. Maerkl and S. R. Quake, *Science*, 2002, **298**, 580.
- 15 T. Thorsen, R. W. Roberts, F. H. Arnold and S. R. Quake, *Phys. Rev. Lett.*, 2001, **86**, 4163.
- 16 H. Song, D. L. Chen and R. F. Ismagilov, *Angew. Chem., Int. Ed. Engl.*, 2006, **45**, 7336.
- 17 B. Zheng, L. S. Roach and R. F. Ismagilov, *J. Am. Chem. Soc.*, 2003, **125**, 11170.
- 18 J. Shim, G. Cristobal, D. Link, T. Thorsen and S. Fraden, *Using microfluidics to decouple nucleation and growth of protein crystals*, 2006, <http://www.elsie.brandeis.edu/JACS2006/JACS2006.html>.
- 19 P. Laval, J.-B. Salmon and M. Joanicot, *J. Cryst. Growth*, 2007, DOI: 10.1016/j.jcrysgro.2006.12.044.
- 20 J. C. McDonald and G. M. Whitesides, *Acc. Chem. Res.*, 2002, **35**, 491.
- 21 S. L. Anna, N. Boutoux and H. A. Stone, *Appl. Phys. Lett.*, 2003, **82**, 364.
- 22 G. Cristobal, L. Arbouet, F. Sarrazin, D. Talaga, J.-L. Bruneel, M. Joanicot and L. Servant, *Lab Chip*, 2006, **6**, 1140.
- 23 B. T. Lau, C. A. Baitz, X. P. Dong and C. L. Hansen, *J. Am. Chem. Soc.*, 2007, **129**, 454.
- 24 A. C. Zettlemoyer, *Nucleation*, Marcel Dekker, New York, 1969.
- 25 D. Kashchiev and G. M. Rosmalen, *Cryst. Res. Technol.*, 2003, **38**, 555.
- 26 J. W. Mullin, *Crystallization*, Butterworth-Heinemann, Oxford, 4th edn, 2001.
- 27 A. Apelblat and E. Manzurola, *J. Chem. Thermodyn.*, 1986, **19**, 317.
- 28 J. Leng, B. Lonetti, P. Tabeling, M. Joanicot and A. Ajdari, *Phys. Rev. Lett.*, 2006, **96**, 084503.



Looking for that **special** research paper from applied and technological aspects of the chemical sciences?

TRY this free news service:

Chemical Technology

- highlights of newsworthy and significant advances in chemical technology from across RSC journals
- free online access
- updated daily
- free access to the original research paper from every online article
- also available as a free print supplement in selected RSC journals.*

*A separately issued print subscription is also available.

Registered Charity Number: 207890

22030683

RSC Publishing

www.rsc.org/chemicaltechnology